

Quantitative and Anatomical Imaging of Human Skin by Noninvasive Photoacoustic Dermoscopy

Zhiyang Wang^{1,2}, Fei Yang^{1,2}, Wuyu Zhang^{1,2,3} and Sihua Yang^{1,2} *

¹MOE Key Laboratory of Laser Life Science and Institute of Laser Life Science, College of Biophotonics, South China Normal University, Guangzhou, China

²Guangdong Provincial Key Laboratory of Laser Life Science, College of Biophotonics, South China Normal University, Guangzhou, China

³Guangdong Photoacoustic Medical Technology Co., Ltd., Guangzhou, China

*For correspondence: yangsh@scnu.edu.cn

Abstract

Imaging plays a vital role in the diagnosis and treatment of skin diseases. However, pure optical imaging technique is limited to the visualization of superficial skin tissues. Ultrasonic imaging technique can detect deep tissues, but it lacks detailed information on microscopic pathological structures. Photoacoustic imaging is an advanced technology that bridges the spatial-resolution gap between optical and ultrasonic techniques, by the modes of optical excitation and acoustic detection. Photoacoustic dermoscopy (PAD), based on photoacoustic technology, can noninvasively obtain high-resolution anatomical structures by endogenous absorbers, such as melanin, hemoglobin, lipids, etc. In the past years, PAD has gradually been developed in clinical dermatology for the diagnosis of melanoma, psoriasis, port-wine stains, dermatitis, skin grafting, and testing the efficacy of cosmetics. This protocol provides detailed procedures for PAD construction, including component selection, equipment setup, and system calibration. A step-by-step guide for human skin imaging is provided as an example application. Image reconstruction and troubleshooting procedures are also elaborated. PAD offers the 3D volumetric images of human skin, and quantitatively analyzes the vascular morphology in the dermis. The protocol will provide clinicians with standardized and reasonable guidance in dermatological imaging.

Keywords: Biomedical imaging, Photoacoustics, Dermoscope, Human skin, Quantitative imaging

This protocol was validated in: J Eur Acad Dermatol Venereol (2021), DOI: 10.1111/jdv.17677

Background

The skin is the largest organ of the human body. The state of the skin is closely related to human health. Imaging technology plays an important role in dermatology. Conventional pure optical dermatoscopes are limited by imaging depth and can only visualize epidermal morphology. Ultrasound imaging can visualize the entire skin structure with deep penetration, but its spatial resolution and ability to visualize microvessels are relatively poor. Photoacoustic imaging (PAI), based on the photoacoustic effect, is a hybrid biomedical imaging technology, which combines high-contrast optical imaging and deep penetration ultrasound imaging (Wang and Hu, 2012). As a meritorious application mode of PAI, photoacoustic dermoscopy (PAD) provides researchers and clinicians with a new way of noninvasively observing deep skin structures (Xu *et al.*, 2016; Ma *et al.*, 2018, 2020, 2021; Wang *et al.*, 2022a, 2022b). PAD overcomes the strong photon scattering caused by the skin tissue's multilayered structures and complex heterogeneous medium, and achieves full-thickness imaging of human skin with high resolution (Wang *et al.*, 2022b). Differently configured PADs allow spatial resolution to be scaled to the desired skin imaging depth, while maintaining a high depth-to-resolution ratio. By depicting the fine anatomical structures from epidermis to subcutaneous tissue, PAD can be used to diagnose abnormal pigmentation, and vascular malformation. PAD is gradually proposed in clinical dermatology for the diagnosis of melanoma, psoriasis, port-wine stains, dermatitis, skin grafting, and for the assessment of the efficacy of cosmetics (Aguirre *et al.*, 2017; Tsuge *et al.*, 2020; Wang *et al.*, 2022a). In clinical diagnosis and treatment, quantitative information on the distribution, depth, and diameter of the melanin and vessels can be obtained to determine optimum treatment parameters for individual patients. Currently, the limitation of PAD lies in the fact that coupling gel is required to transmit photoacoustic signals, which is not conducive to imaging skin ulcers. In the future, non-contact photoacoustic detection technology could make up for this deficiency. This protocol is dedicated to the design and debugging of PAD for human skin imaging. Overall, this protocol will promote preclinical and clinical applications of PAD in dermatology and plastic surgery.

Materials and Reagents

1. Polyethylene membrane (He Jian Jie Li Plastic Products Co., Ltd., membrane thickness: 10 μm)
2. Ultrasound gel (GUANGGONG PAI, medical ultrasound gel)
3. Deionized water

Equipment

1. FiberPort (Thorlab, model: PAF-X-7-A)
2. Single-mode fiber (Thorlab, model: P1-460B-FC-5)
3. Collimator (Thorlab, model: F240FC-532)
4. Objective lens (Daheng Optics, model: GCO-2101)
5. Ultrasonic transducer (Doppler Electronic Technology, model: Focused $\phi 8-3$)
6. Amplifier (RF Bay, model: LNA-650)
7. Data acquisition card (Spectrum, model: M3i.3221)
8. Graphics Processing Unit (NVIDIA, model: GeForce GTX 1060)
9. X-Y translation stage (Jiancheng Optics, model: LS2-25T)
10. Motor driver (Jiancheng Optics, model: LS2-MD)
11. Robot arm (Ergotron, model: 826-842)
12. Field Programmable Gate Array (Altera, model: Cyclone IV)
13. Coupling cup (Shenzhen WeNext Technology, material: nylon)
14. Coaxial cable (Talent RG cable, model: RG58/U)
15. SubMiniature version A (SMA) connector (Rebes, model: 50 Ω)
16. Laser goggles (Daheng Optics, model: GCAQ-YAD)

17. Copper foil tape (Shenzhen Sanwangda Electronic Materials, model: 3M1181)
18. Buckle-type magnetic ring (Jia Lin Magnetic Industry, model: SCRC 35B)
19. 532-nm pulsed laser (Laser-export, model: DTL-314QT)
20. DC power supply (LONG WEI, model: PS-1502D)
21. Laser power meter (Phyiscience Opto-electronics, model: LPE-1)
22. Digital multimeter (Fluke, model: 115C)

Software

1. LabVIEW 2016 (National Instruments, <https://www.ni.com/zh-cn.html>)
2. MATLAB2020a (MathWorks, <https://ww2.mathworks.cn/>)
3. ImageJ (National Institutes of Health software, <https://imagej.nih.gov/ij/>)

Procedure

This protocol is adapted from Wang *et al.* (2022b), and provides the detailed procedures for PAD construction, including component selection, equipment setup, and system calibration. A step-by-step guide for human skin imaging is provided as an example application.

A. System setup

1. Use a 532-nm pulsed laser as the laser illumination source. Set the repetition rate of the laser to 10 kHz, the output energy to 80%, and the trigger setting to external trigger using a LabVIEW program (Figure 2A).

Note: The laser is a class IV laser. Wear laser protection goggles during operation.

2. Fix the FiberPort directly in front of the laser beam exit port (Figure 2B).
3. Couple the laser beam to the single-mode fiber (SMF) by a FiberPort (FP) (Figure 2B).

Note: Keep the lens of the FiberPort and fiber end face clean.

4. Use a fiber collimator to collimate the laser beam at the output of the single-mode fiber (Figure 2C).
5. Use the objective lens to focus the collimated laser beam (Figure 2D).
6. Fix the ultrasonic transducer under the objective lens (Figure 2E).
7. Pass the focused laser beam through the center hole of the ultrasonic transducer (Figure 2F).
8. Fix the coupling cup under the ultrasonic transducer (Figure 2G).

Note: Use a housing to fix the collimator, objective lens, ultrasonic transducer, and coupler coaxially up and down one by one, as shown in Figure 1A.

9. Fix the housing in the center of the X-Y translation stage.
10. Connect the ultrasonic transducer to the input port of the amplifier (Figure 2H).
11. Use a coaxial cable to connect the output port of the amplifier to the input port of the data acquisition card.
12. Set the DC power supply to 15 V, to power the amplifier.
13. Use a coaxial cable with SMA connector to connect the output port of the motor driver to the I/O port1 of

- the FPGA (Figure 2I).
14. Use a coaxial cable with SMA connector to connect the I/O port2 of the FPGA to the external trigger of the pulsed laser (Figure 2I).
 15. Use a coaxial cable with SMA connector to connect the I/O port3 of the FPGA to the external trigger of the data acquisition card, to input the synchronous signals (Figure 2J).

Note: Timing diagram of I/O ports are shown in Figure 1B.

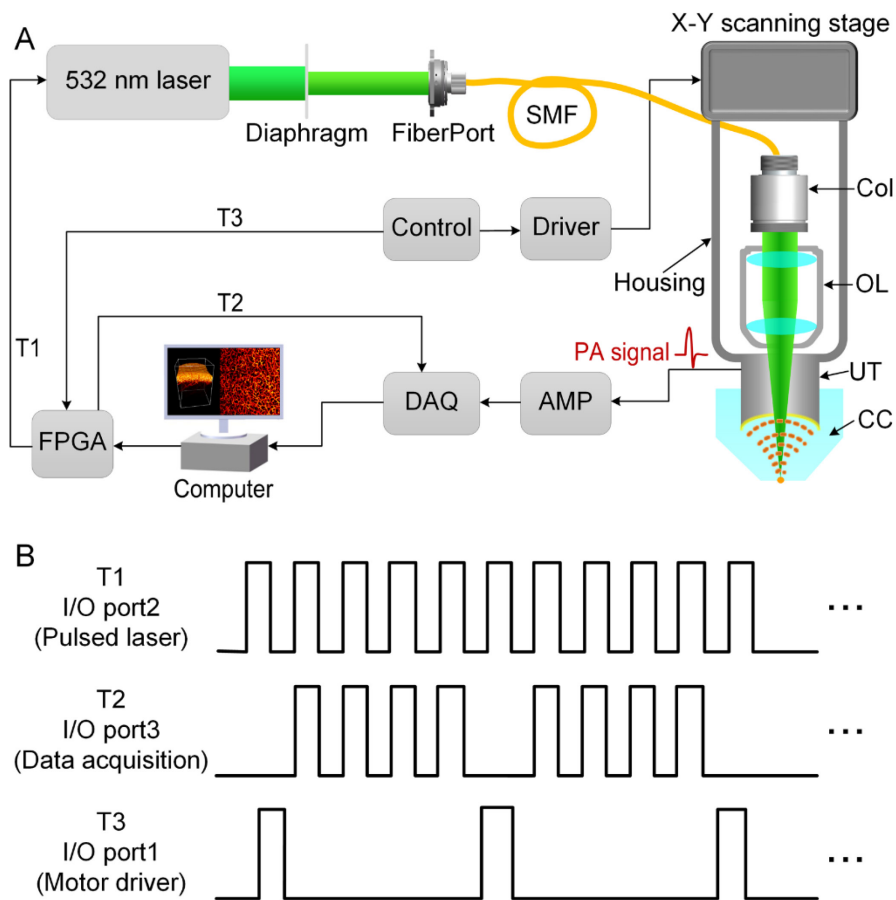


Figure 1. Photoacoustic dermoscopy system setup.

A. Schematic diagram of the PAD system. B. Timing diagram of scanning and acquisition. T1, T2, T3: trigger; Col: collimator; OL: objective lens; UT: ultrasonic transducer; CC: coupling cup; SMF: single-mode fiber; DAQ: data acquisition card; AMP: amplifier; FPGA: field programmable gate array.

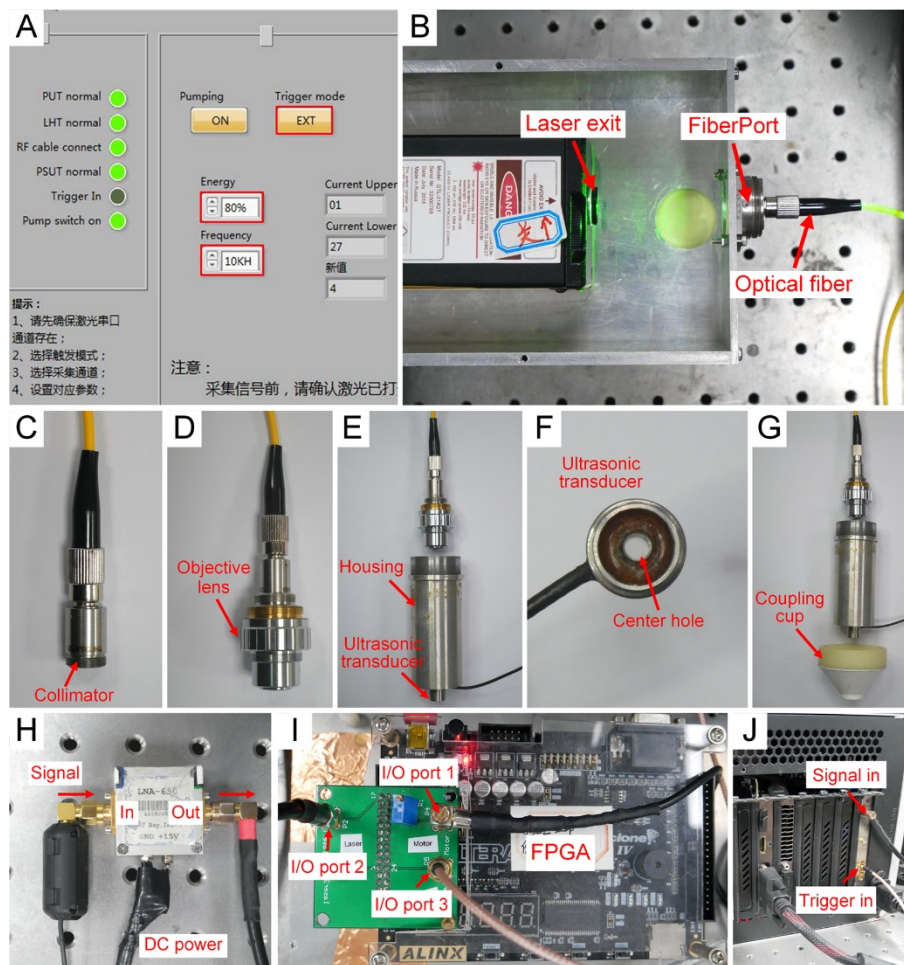


Figure 2. System alignment pictures.

A. LabVIEW program for laser. B. Laser and fiberPort. C. Fiber collimator. D. Objective lens. E. Housing and ultrasonic transducer. F. Coupling cup. G. Ultrasonic transducer. H. Signal from ultrasonic transducer to amplifier. I. Trigger connections on FPGA. J. Trigger and signal connections on data acquisition card.

B. System alignment

1. Use a polyethylene membrane to seal the bottom of the coupling cup, and add deionized water to the coupling cup (Figure 3A).
2. Add deionized water below the ultrasonic transducer (Figure 3B).
3. Adjust the bottom of the ultrasonic transducer into the deionized water (Figure 3C).

Note: Avoid bubbles in the bottom part of the ultrasonic transducer.

4. Open the laser switch. Select the laser control program. Preheat for fifteen minutes.

Note: The laser is a class IV laser. Wear laser protection goggles during operation.

5. Press the “ON” button for the pumping switch. Set the external trigger for the pulsed laser.
6. Carefully check the laser pulse energy and the pulse repetition rate.

7. Use the laser power meter to measure the light energy, to ensure a safety threshold (20 mJ/cm²).
8. Place a blade on the bottom of the polyethylene membrane.

Note: Apply ultrasound gel between the blade and the membrane, and avoid bubbles.

9. Select the A-Line LabVIEW program. Press the “Start” button to capture the fixed-point signal and display the amplitude and the spectrum of the current A-Line signal.
10. Adjust the X-Y position of the ultrasonic transducer to avoid signal oscillation, and make sure the optical and acoustic foci are confocal.
11. Adjust the height of the coupling cup, to maximize the amplitude of the A-Line signal (Figure 3C).
12. Remove the blade and wipe the ultrasound gel on the polyethylene membrane.
13. Add the ultrasound gel on the skin of the volunteer and apply it evenly.
14. Place the integrated imaging probe close to the skin of the volunteer and capture the A-Line signal of the human skin *in vivo*.
15. Adjust the height of the coupling cup slightly, to maximize the amplitude of the skin signal.

Note: The normal PA signal is shown in Figure 2D.

16. Stop the A-Line LabVIEW program.

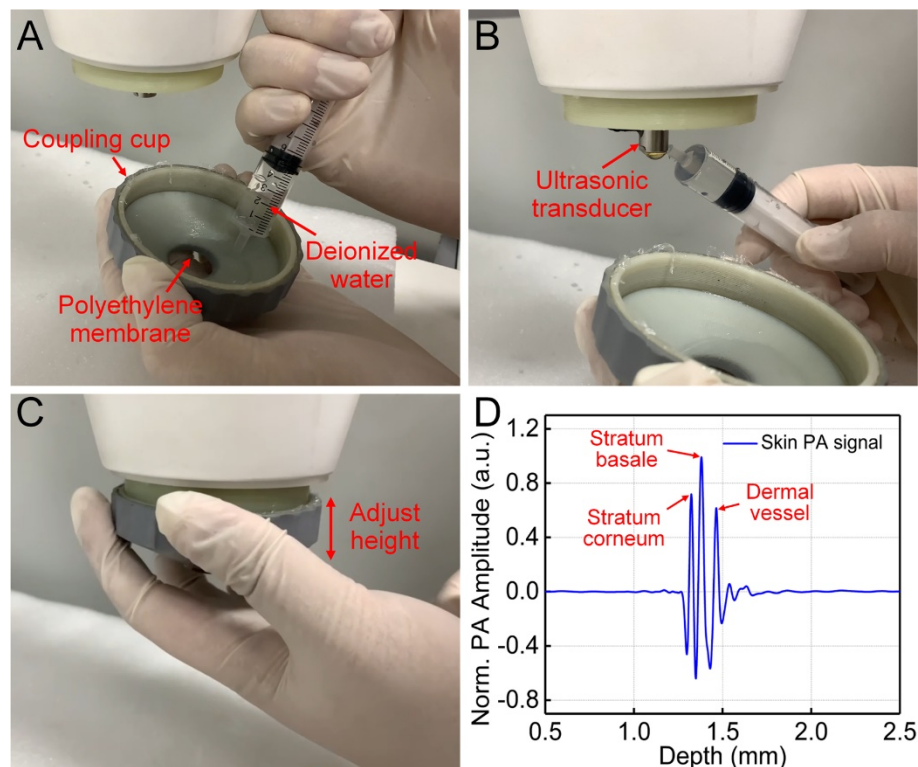


Figure 3. System alignment and acquisition of skin signals.

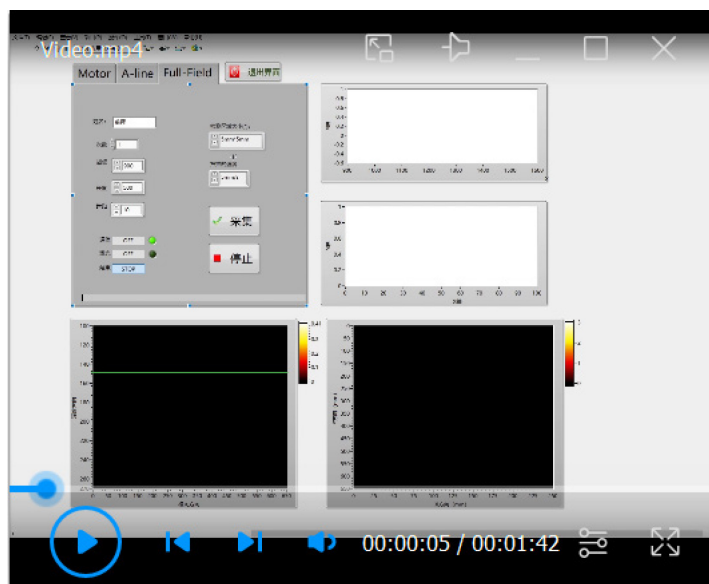
A. Add deionized water to the coupling cup. B. Add deionized water below the ultrasonic transducer. C. Adjust the relative height of the coupling cup and the ultrasonic transducer. D. A-Line PA signal of human skin.

C. Human skin imaging (Video 1)

1. Before human skin imaging, oral and written informed consent were obtained from all participants.
2. Participants need to wear laser goggles.
3. Open the laser switch. Select the laser control program. Preheat for fifteen minutes.

Note: The laser is a class IV laser. Wear laser protection goggles during operation.

4. Press the “ON” button for the pumping switch. Set the external trigger for the pulsed laser.
5. Carefully check the laser pulse energy and the pulse repetition rate.
6. Select the imaging region and apply ultrasound gel or deionized water (Figure 4A).
7. Press the polyethylene membrane of the coupling cup fully in contact with the skin imaging area (Figure 4B).
8. Open the LabVIEW program. Name the newly created folder to save the data.
9. Select the scanning speed, the size of the scanning area, the scanning step, and the acquisition depth. For example, set the scanning parameter at “10 mm/s” in the “Speed” tab, “5 mm*5 mm” in the “Area” tab, “500” in the “acquisition depth” tab, and “10” in the “Step” tab.
10. Click the “Collect” button to start scanning.
11. Keep the volunteer still and avoid physical movement.
12. Click the “Stop” button to end scanning after completing scanning. Click the “Return to Zero” to make the X-Y translation stage return to zero.
13. Press the "OFF" button to turn off the laser.
14. Click the “Exit” button to exit the LabVIEW program.
15. Remove the polyethylene membrane and pour out the deionized water in the coupling cup.



Video 1. Human skin imaging

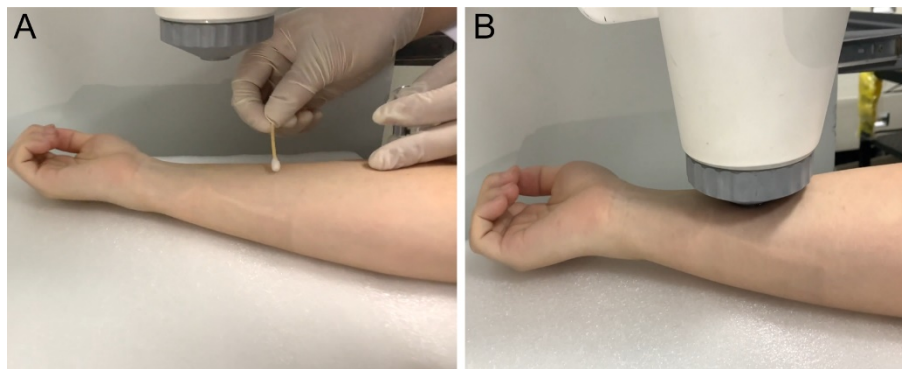


Figure 4. System alignment and acquisition of skin signals.

A. Apply ultrasound gel or deionized water to the target region before imaging. B. Keep the coupling cup fully in contact with the skin.

D. Troubleshooting procedures

1. Larger laser spot or inhomogeneous illumination: First, make sure that the fiber collimator is correctly connected to the output end of the single-mode fiber. Second, make sure that there are no air bubbles under the ultrasonic transducer.
2. No PA signals: First, make sure that the Data acquisition card can collect signals normally. If the Data acquisition card does not work, please check whether the external trigger signal is normal. Second, make sure that the pulsed laser is set to external trigger. Third, make sure that the amplifier is powered, and that all coaxial cables are functioning properly and connected correctly.
3. Strong external noise in the PA signal: First, use the digital multimeter to ensure that the ground wires of the motor driver, amplifier, and ultrasonic transducer are connected to the ground wire of the power supply. Second, use copper foil tape to connect the amplifier to the housing. Third, fix the buckle-type magnetic ring on the SMA connector of the amplifier and the coaxial signal cable.
4. Strong motion artifact in the PA image: First, make sure that the robot arm is fixed and stable. Second, make sure that the X-Y translation stage and housing are rigidly connected.

Data analysis

1. Each laser pulse produces a one-dimensional (1D) depth-resolved image without mechanical scanning, while 2D transverse scanning generates a 3D image. The 3D volume PA data are obtained after scanning the skin (Figure 5A). For PA data treatment, first, the skin morphology is observed to obtain skin surface (red dashed lines as seen in Figure 5B), through the x - z cross-sectional images. Then, according to the skin surface and thickness of the stratum corneum and stratum basale, all x - z cross-sectional images are divided according to their depth, to obtain the stratum corneum, the stratum basale, and the dermis. The depth of melanin and hemoglobin distributions are clearly visualized in the PA cross-sectional image. Figures 5B1–5B3 respectively represent the PA cross-sectional images of the stratum corneum, the stratum basale, and the dermis. Furthermore, the lateral maximum amplitude projections (MAPs) of these structures are shown in Figures 5C–5E, which clearly demonstrate distinct morphological structures in different skin layers. Figure 5E shows the abundant vascular morphology in the dermis; the branching and morphology of this microvasculature is closely related to the physiological condition of human skin (Aguirre *et al.*, 2017).

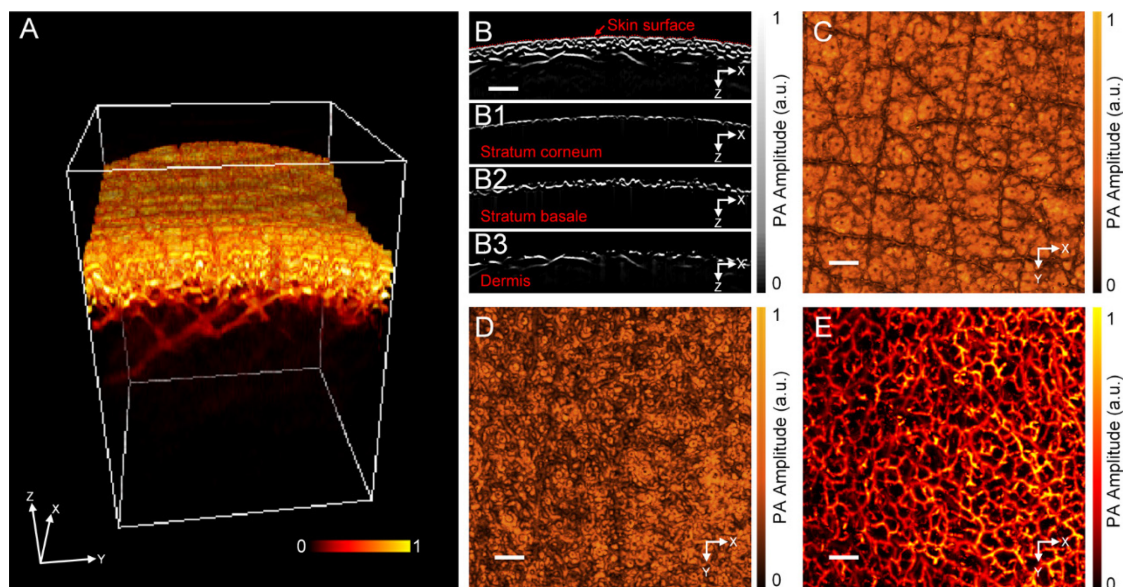


Figure 5. *In vivo* imaging of human skin.

A. 3D volumetric image of human skin. B. PA cross-sectional image of human skin, with B1. the stratum corneum, B2. the stratum basale, and B3. the dermis layers. C–D. Photoacoustic lateral MAP images of C. the stratum corneum, D. the stratum basale., and E. the dermis. Scale bar: 0.5 mm. PA, photoacoustic; MAP, maximum amplitude projection.

- To further quantify vascular morphology, analyze the density and diameter of blood vessels in the dermis (Figure 6A). The vessel density (VD) is defined as the ratio of all blood vessel pixels to the total pixels of the selected total area, to reflect the amount of blood vessel distribution in a given region. Among them, the overall pixels are the total number of pixels in the selected area, and the vessel pixels are the total number of pixels of blood vessels in the area.

To calculate the density of blood vessels, first change the image format to 8-bit (Menu: Image, Type, 8-bit), set a suitable threshold, and binarize the photoacoustic image (Menu: Image, Adjust, Threshold). In the corresponding binary image, the vascular pixel gray value is set to 1, and the non-vascular pixel gray value is set 0 (Figure 6B). Finally, the ratio of the number of vessel pixels to the number of all pixels is calculated: vessel density is ~37%.

For calculation of the vascular diameter, a vertical line passing through the vascular skeleton intersects the vascular boundary at two points, and the distance between these two points is considered the diameter of the vessel at that point. First, binarize the photoacoustic image, and then extract the boundaries of the vessels (Figure 6C). Draw a vertical line of each pixel point of the skeleton of the blood vessel within a certain range around the pixel point. The corresponding two points in the blood vessel boundary map are determined, and the linear distance between the two points is calculated as the diameter at the point. Finally, plot the statistical histogram of vascular diameter (Figure 6D).

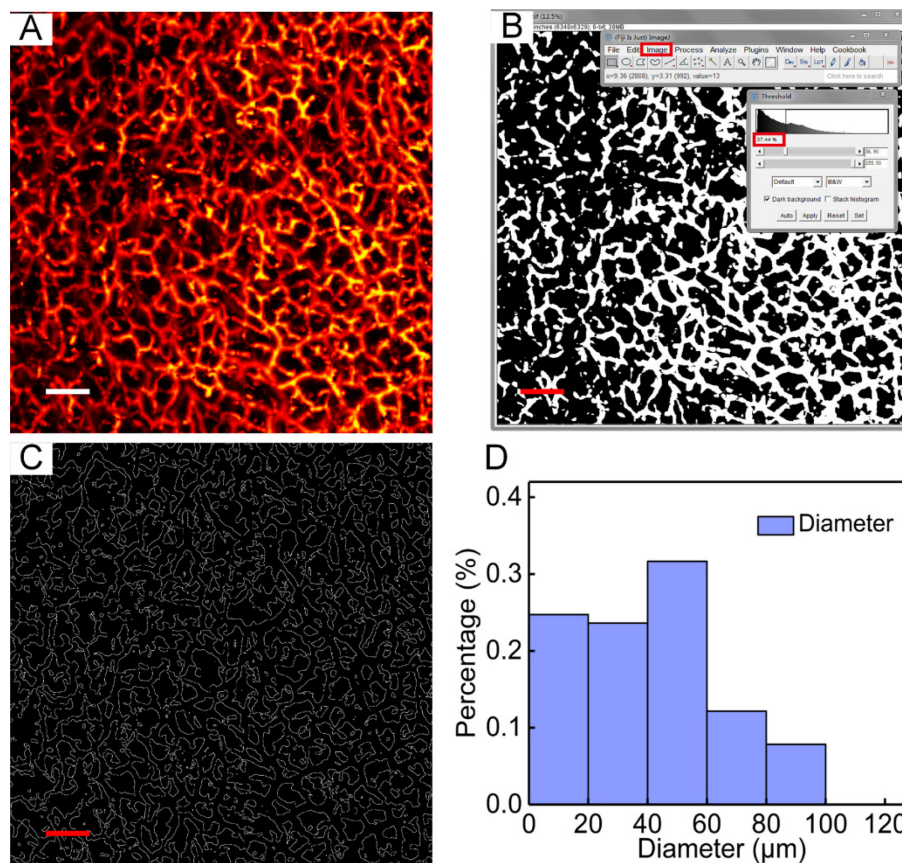


Figure 6. Quantitative assessment of skin vascular morphology.

A. Photoacoustic lateral MAP images of dermis. B. The binary image corresponding to A. C. The boundaries of the vessels corresponding to A. D. Distribution of the vessel diameter in A. Scale bar: 0.5 mm.

Notes

1. The amplifier power supply is adjusted to 15 V, as higher voltage will damage the amplifier.
2. The laser energy used to irradiate the human skin needs to meet safety standards (American National Standard for Safe Use of Lasers).

Acknowledgments

Funding: This work was supported by National Natural Science Foundation of China (61822505; 11774101), the Science and Technology Planning Project of Guangdong Province, China (2015B020233016), and the Science and Technology Program of Guangzhou (2019050001).

This protocol was adapted from a previous study from our laboratory published in Journal of the European Academy of Dermatology and Venereology (Wang *et al.*, 2022b), and Quantitative Imaging in Medicine and Surgery (Wang *et al.*, 2022a).

Competing interests

The authors have no conflicts of interest or competing interests to declare.

Ethics

The study was approved by the Chinese Ethics Committee of Registering Clinical Trials (ChiECRCT20200184) and registered with Chinese Clinical Trial Registry (ChiCTR2000034400). Before skin imaging, written informed consent was taken from all individual participants.

References

- Aguirre, J., Schwarz, M., Garzorz, N., Omar, M., Buehler, A., Eyerich, K. and Ntziachristos, V. (2017). [Precision assessment of label-free psoriasis biomarkers with ultra-broadband optoacoustic mesoscopy](#). *Nat Biomed Eng* 1(5): 0068.
- Ma, H., Cheng, Z., Wang, Z., Gu, Y., Zhang, T., Qiu, H. and Yang, S. (2018). [Fast linear confocal scanning photoacoustic dermoscopy for non-invasive assessment of chromatodermatosis](#). *Appl Phys Lett* 113: 083704.
- Ma, H., Cheng, Z., Wang, Z., Zhang, W. and Yang, S. (2020). [Switchable optical and acoustic resolution photoacoustic dermoscope dedicated into *in vivo* biopsy-like of human skin](#). *Appl Phys Lett* 116(7): 073703.
- Ma, H., Cheng, Z., Wang, Z., Qiu, H., Shen, T., Xing, D., Gu, Y. and Yang, S. (2021). [Quantitative and anatomical imaging of dermal angiopathy by noninvasive photoacoustic microscopic biopsy](#). *Biomed Opt Express* 12(10): 6300-6316.
- Tsuge, I., Saito, S., Yamamoto, G., Sekiguchi, H., Yoshikawa, A., Matsumoto, Y., Suzuki, S. and Toi, M. (2020). [Preoperative vascular mapping for anterolateral thigh flap surgeries: A clinical trial of photoacoustic tomography imaging](#). *Microsurgery* 40(3): 324-330.
- Wang, L. V. and Hu, S. (2012). [Photoacoustic tomography: *in vivo* imaging from organelles to organs](#). *Science* 335(6075): 1458-1462.
- Wang, Z., Yang, F., Ma, H., Cheng, Z. and Yang, S. (2020). [Photoacoustic and ultrasound \(PAUS\) dermoscope with high sensitivity and penetration depth by using a bimorph transducer](#). *J Biophotonics* 13(9): e202000145.
- Wang, Z., Yang, F., Cheng, Z., Zhang, W., Xiong, K., Shen, T. and Yang, S. (2022a). [Quantitative multilayered assessment of skin lightening by photoacoustic microscopy](#). *Quant Imaging Med Surg* 12(1): 470-480.
- Wang, Z., Yang, F., Ma, H., Cheng, Z., Zhang, W., Xiong, K., Shen, T. and Yang, S. (2022b). [Bifocal 532/1064 nm alternately illuminated photoacoustic microscopy for capturing deep vascular morphology in human skin](#). *J Eur Acad Dermatol Venereol* 36(1): 51-59.
- Xu, D., Yang, S., Wang, Y., Gu, Y. and Xing, D. (2016). [Noninvasive and high-resolving photoacoustic dermoscopy of human skin](#). *Biomed Opt Express* 7(6): 2095-2102.